Stritt, S., Nurden, P., Turro, E., Greene, D., Jansen, S. B., Westbury, S. K., Petersen, R., Astle, W. J., Marlin, S., Bariana, T. K., Kostadima, M., Lentaigne, C., Maiwald, S., Papadia, S., Kelly, A. M., Stephens, J. C., Penkett, C. J., Ashford, S., Tuna, S., ... Mumford, A. D. (2016). A gain-of-function variant in *DIAPH1* causes dominant macrothrombocytopenia and hearing loss. *Blood*, *127*(23), 2903-2914. https://doi.org/10.1182/blood-2015-10-675629

A gain-of-function *DIAPH1* variant causes dominant macrothrombocytopenia and hearing loss

Running title: *DIAPH1* and macrothrombocytopenia

Authors: Simon Stritt[1*], Paquita Nurden[2,3*], Ernest Turro[4-7,*], Daniel Greene[4,6,7], Sjoert B Jansen[4,5], Sarah K Westbury[8], Romina Petersen[4,5], William J Astle[4-6], Sandrine Marlin[9], Tadbir K Bariana[10,11], Myrto Kostadima[4,5], Claire Lentaigne[12,13], Stephanie Maiwald[4,5], Sofia Papadia[4,7], Anne M Kelly[4,5], Jonathan C Stephens[4,5], Christopher J Penkett[4,7], Sofie Ashford[4,7], Salih Tuna[4,7], Steve Austin[14], Tamam Bakchoul[15], Peter Collins[16], Rémi Favier[17], Michele P Lambert[18,19], Mary Mathias[20], Carolyn M Millar[12,13], Rutendo Mapeta[4,7], David J Perry[21], Sol Schulman[22], Ilenia Simeoni[4,7], Chantal Thys[23], BRIDGE-Bleeding and Platelet Disorders (BPD) Consortium[#], Keith Gomez[11], Wendy N Erber[24], Kathleen Stirrups[4,7], Augusto Rendon[25], John R Bradley[5,26], Chris van Geet[23], F Lucy Raymond[7,27], Michael A Laffan[12,13], Alan T Nurden[2,3], Bernhard Nieswandt[1], Sylvia Richardson[6], Kathleen Freson[23*], Willem H Ouwehand[4,5,7,28,*], Andrew D Mumford[29*]

Affiliations: [1] Department of Experimental Biomedicine, University Hospital and Rudolf Virchow Center, University of Würzburg, Würzburg, Germany, [2] Institut Hospitalo-Universitaire LIRYC, PTIB, Hôpital Xavier Arnozan, Pessac, France. [3] French Reference Center on Inherited Platelet Disorders, CHU Timone, Marseille, France. [4] Department of Haematology, University of Cambridge, Cambridge Biomedical Campus, Cambridge, United Kingdom. [5] NHS Blood and Transplant, Cambridge Biomedical Campus, Cambridge, United Kingdom. [6] Medical Research

Council Biostatistics Unit, Cambridge Institute of Public Health, Cambridge Biomedical Campus, Cambridge, United Kingdom. [7] NIHR BioResource - Rare Diseases, Cambridge University Hospitals, Cambridge Biomedical Campus, Cambridge, United Kingdom. [8] School of Clinical Sciences, University of Bristol, United Kingdom. [9] Centre de Référence des Surdités Génétiques, Service de Génétique Médicale, Hôpital Necker-Enfants Malades, AP-HP, Paris, France. [10] Department of Haematology, University College London Cancer Institute, London, United Kingdom. [11] The Katharine Dormandy Haemophilia Centre and Thrombosis Unit, Royal Free London NHS Foundation Trust, London, United Kingdom. [12] Centre for Haematology, Hammersmith Campus, Imperial College Academic Health Sciences Centre, Imperial College London, London, United Kingdom. [13] Imperial College Healthcare NHS Trust, Du Cane Road, London, United Kingdom. [14] Department of Haematology, Guy's and St Thomas' NHS Foundation Trust, London, United Kingdom. [15] Institute for Immunology and Transfusion Medicine, Universitätsmedizin Greifswald, Germany. [16] Arthur Bloom Haemophilia Centre, Institute of Infection and Immunity, School of Medicine, Cardiff University, United Kingdom. [17] Assistance Publique - Hôpitaux de Paris, Armand Trousseau Children Hospital, Paris, Inserm U1170, Villejuif, France. [18] Division of Hematology, Children's Hospital of Philadelphia, Philadelphia, United States of America. [19] Department of Pediatrics, Perelman School of Medicine at the University of Pennsylvania, Philadelphia, United States of America. [20] Department of Haematology, Great Ormond Street Hospital for Children NHS Foundation Trust, London, United Kingdom. [21] Department of Haematology, Addenbrooke's Hospital, Cambridge University Hospitals NHS Foundation Trust, Cambridge Biomedical Campus, Cambridge, United Kingdom. [22] Beth Israel Deaconess Medical Centre, Harvard Medical School, Boston, United States of America. [23] Department of

Cardiovascular Sciences, Center for Molecular and Vascular Biology, University of Leuven, Belgium. [24] Pathology and Laboratory Medicine, University of Western Australia, Crawley, Western Australia, Australia. [25] Genomics England Ltd, London, United Kingdom. [26] Research & Development, Cambridge University Hospitals NHS Foundation Trust, Cambridge, United Kingdom. [27] Department of Medical Genetics, Cambridge Institute for Medical Research, University of Cambridge, Cambridge, United Kingdom. [28] Human Genetics, Wellcome Trust Sanger Institute, Wellcome Trust Genome Campus, Hinxton, Cambridge, United Kingdom. [29] School of Cellular and Molecular Medicine, University of Bristol, Bristol, United Kingdom.

* Authors contributed equally to the study

A list of additional members of the BRIDGE-BPD Consortium is provided in supplementary information**.**

Number of words: total 3909; abstract 171

Number of figures and tables: 9

Number of references: 45

Corresponding authors:

Dr Ernest Turro, Department of Haematology, University of Cambridge & NHS Blood and Transplant, Long Road, Cambridge, CB2 0PT. UK;

Tel +44 (0) 1223 588 727; email et341@cam.ac.uk

Dr Kathleen Freson, Department of Cardiovascular Sciences, Center for Molecular and Vascular Biology, University of Leuven, Belgium; Tel +32 (0) 16 341707; email Kathleen.Freson@med.kuleuven.be

Scientific category: Platelets and thrombopoiesis

KEY POINTS

A gain-of-function variant in *DIAPH1* is the basis of a new human syndromic disorder of macrothrombocytopenia and sensorineural hearing loss

Our observations of altered megakaryopoiesis and platelet cytoskeletal regulation highlight a critical role for DIAPH1 in platelet formation

ABSTRACT

Macrothrombocytopenia (MTP) is a heterogeneous group of disorders characterised by enlarged and reduced numbers of circulating platelets, sometimes resulting in abnormal bleeding. In most MTP, this phenotype arises because of altered regulation of platelet formation from megakaryocytes (MK). We report the identification of *DIAPH1,* which encodes the Rho-effector diaphanous-related formin 1 (DIAPH1), as a candidate gene for MTP using exome sequencing, ontological phenotyping and similarity regression. We describe two unrelated pedigrees with MTP and sensorineural hearing loss that segregate with a *DIAPH1* p.R1213* variant predicting partial truncation of the DIAPH1 diaphanous autoregulatory domain. The R1213* variant was associated with reduced proplatelet formation from cultured MK, cell clustering and abnormal cortical filamentous actin. Similarly, in platelets there was increased filamentous actin and stable microtubules, indicating constitutive activation of DIAPH1. Over-expression of DIAPH1 R1213* in cells reproduced the cytoskeletal alterations found in platelets. Our description of a novel syndromic disorder of platelet formation and hearing loss extends the repertoire of characterised human MTP and provides new insights into the autoregulation of DIAPH1 activity.

INTRODUCTION

Platelet formation by megakaryocytes (MKs) requires an ordered sequence of differentiation steps from haematopoietic stem cells followed by MK maturation, during which repeated rounds of DNA replication without cell division usually result in very large MKs with a single nucleus and DNA contents up to 128N. This process enables the accumulation of platelet-specific granules and a demarcation membrane system that will later contribute to the platelet cytoplasmic contents and surface membrane.[1, 2] Platelets are generated from mature MKs by the protrusion of cytoplasmic extensions termed proplatelets into bone marrow sinusoids, where final platelet sizing and shaping occurs.[3] Platelet formation strongly depends on microtubules, which enable proplatelet elongation and transport of organelles from the MK cytoplasm, [1] and actin-dependent processes, which mediate the branching of elongating proplatelets, thereby determining the number of available proplatelet tips to form platelets.[4]

Altered regulation of platelet formation is a feature of several human hematopoietic disorders, including macrothrombocytopenia (MTP) in which there are enlarged and reduced numbers of circulating platelets, sometimes resulting in abnormal bleeding.[5, 6] MTP has been associated with pathogenic variants in genes that regulate MK maturation (*GATA1*, *GFI1B* and *NBEAL2)* or which encode platelet surface proteins (*GP1BA*, *GP1BB*, *GP9*, *ITGA2B* and *ITGB3*; reviewed in [5]). However, a prevalent sub-group of MTP arise from variants in *ACTN1*,[7] *FLNA*,[8] *MYH9*,[9, 10] *TUBB1*,[11] and *PRKACG*[12] which encode MK cytoskeletal proteins or interactors. It has been proposed that the platelet phenotype associated with some *MYH9,*[13, 14] *ACTN1,*[7] and *TUBB1*[15] variants results from aberrant cytoskeletal rearrangements during proplatelet formation, leading to altered platelet production. Cytoskeletal dysfunction may also

underlie associated phenotypes such as hearing loss, cataract and glomerulopathy with some *MYH9* variants [10, 16] and periventricular nodular heterotopia and otopalatodigital syndromes with some *FLNA* variants.[8]

Here we extend the repertoire of MTP by reporting the discovery of a new dominant syndromic disorder of platelet formation. We show that MTP was associated with sensorineural hearing loss in two unrelated pedigrees and that this phenotype segregates with the same chain-truncating variant in *DIAPH1*, which encodes the cytoskeletal regulator and Rho-effector, diaphanous-related formin 1 (DIAPH1, mDia1), identified previously as a regulator of megakaryocytopoiesis *in vitro.* [17]

METHODS

Recruitment of cases and genetic analysis.

The cases were enrolled to the BRIDGE-BPD study (UK REC10/H0304/66) or French 'Network on the inherited diseases of platelet function and platelet production' (INSERM RBM 04-14) after providing informed written consent. Control groups comprised other cases with bleeding or platelet disorders (BPD) of unknown genetic basis or with unrelated rare disorders enrolled to the NIHR BioResource-Rare Diseases study (UK REC 13/EE/0325). Data collection, human phenotype ontology (HPO) coding and high throughput sequencing were performed as previously reported.[18] Splice site, frameshift, stop-gain/loss or start-loss variants were analysed further if they were less frequent than 1 in 10,000 in the Exome Aggregation Consortium (ExAC) database and 1 in 100 in our in-house database. Candidate genes for BPD were identified by phenotype similarity regression[19] to allow for the high degree of phenotypic and genetic heterogeneity amongst the BPD cases.

Platelet imaging

Fixed peripheral blood smears were stained with May-Grünwald-Giemsa stain (MGG). Transmission electron microscopy was performed on platelets fixed with 2.5% glutaraldehyde. Platelet diameters and surface areas were measured in a minimum of 99 sections for each case using ImageJ as described previously.[8]

Megakaryocyte colony culture and analysis

$CD34^+$ hematopoietic stem cells (HSCs) were isolated from peripheral blood by magnetic cell sorting and differentiated into MK as described previously in plate and liquid cultures.[20, 21] MK-colony forming units (MK-CFU) and MK were visualised by light or confocal microscopy after staining with MMG, phalloidin or anti-CD61 antibodies. Proplatelet formation (PPF) in liquid MK cultures was determined by light microscopy and ploidy by flow cytometry as described previously.[21]

DIAPH1 expression in cell lines

The DIAPH1-R1213* cDNA was generated by site directed mutagenesis of the full-length wild-type *DIAPH1* cDNA and cloned into the pCMV6-Fc-S (Origene, Rockville, MD) mammalian expression vector, before transient transfection into human embryonic kidney (HEK293FT) or adenocarcinomic human alveolar basal epithelial (A549) cells, cultured using standard conditions.

Western blotting and immunofluorescence microscopy

Denatured washed platelet or transfected HEK293FT cell lysates were separated by SDS-PAGE and blotted onto PVDF membranes. The membranes were probed with primary antibodies recognising DIAPH1, DIAPH3, DIAPH2, GAPDH, β-tubulin,

Tyrosinated tubulin (Tyr-tubulin), detyrosinated tubulin (Glu-tubulin) and acetylated tubulin (ac-tubulin).

For confocal microscopy, transfected A549 cells or platelets applied to fibrinogen-coated coverslips were fixed and probed with antibodies recognising tubulin or DIAPH1 as described above. Filamentous actin was stained using phalloidin-Atto647N. Where indicated, platelets were pre-incubated with 10 µM colchicine. Platelets and cells were visualised by confocal microscopy as reported previously.[22]

Microtubule sedimentation and cold-induced disassembly

Polymerised and soluble microtubule fractions were prepared from lysates of resting or colchicine-treated (10 µM) platelets and from resting or SMIFH2-treated (25 µM) transfected HEK293FT cells by centrifugation for 30 min at 100,000 g and 37°C. Microtubule fractions were visualised by Western blot. Microtubules were depolymerised by incubation of platelets at 4°C. Reassembly was allowed by subsequent rewarming at 37°C as previously reported. [22-24]

Detailed methods and uncropped images of Western blots are provided in Supplementary material.

RESULTS

Selection of DIAPH1 as a candidate gene for MTP

We identified *DIAPH1* as a novel candidate gene for MTP by analysing data from 702 index cases with bleeding or platelet disorders of unknown genetic basis recruited to BRIDGE-BPD study of the NIHR Bioresource-Rare Diseases. Control data were

analysed from 3,453 cases with unrelated rare disorders or unaffected pedigree members recruited to other branches of the NIHR Bioresource-Rare Diseases.

There were 1,073 genes for which at least two BPD cases carried a rare variant predicted to have a high impact on gene translation. After phenotype similarity regression analysis of the genes in this group, *DIAPH1* had the highest probability for the model specifying a statistical association between phenotype and genotype for which thrombocytopenia was inferred (mean (γ)=0.81; **Fig. 1a**) The inferred characteristic phenotype for *DIAPH1* primarily comprised the HPO terms "Sensorineural hearing impairment" and "Abnormality of blood and blood-forming tissues", with the latter driven by the terms "Thrombocytopenia" and "Abnormal bleeding" (**Fig. 1b**).

Two index cases from different pedigrees in the BRIDGE-BPD collection (Bordeaux case 17 and Bristol case 21; **Fig. 1c**) harboured the same high-impact variant in *DIAPH1.* This was a heterozygous c.3637C>T transition, annotated relative to the *DIAPH1* isoform ENST00000398557, which encodes the CCDS-annotated DIAPH1 protein (UNIPROT O60610). This predicted substitution of the conserved (PhyloP p=5.25 × 10^{-4}) arginine at amino acid position 1213 with a premature stop codon (R1213*; **Fig. 2**). This variant was not observed in any of the 61,486 exomes in the ExAC database nor in the remaining 4,151 exomes sequenced in-house. Sanger sequencing showed that the R1213* variant was present in six further pedigree members with both MTP and sensorineural hearing loss but was absent in three asymptomatic pedigree members, indicating segregation with the *DIAPH1* genotype (p=3.66 × 10^{-4}, conditional on the genotypes of the index cases; **Fig. 1c**). We found no

other rare variants shared by the index cases within 10 Mb around *DIAPH1.* The sequencing data provided no evidence that these cases were closely related at genome-wide level or more locally within the *DIAPH1*-containing chromosome 5 (**Supplementary Fig. 1**).

The R1213* variant predicts DIAPH1 protein truncation.

DIAPH1 is a homodimeric formin family protein that promotes actin assembly and regulates microtubule stability through a formin homology (FH) 1 domain which contains binding sites for profilin, and an FH2 domain which promotes nucleation and elongation of actin filaments and possibly microtubule interactions.[25-27] DIAPH1 is regulated by a diaphanous auto-regulatory domain (DAD) near the carboxyl terminus, which inhibits DIAPH1 activity through an interaction with the diaphanous inhibitory domain (DID) near the amino terminus (**Fig. 2**). Auto-inhibition is normally released by competitive binding of activated Rho GTPases, enabling cytoskeletal remodelling. [28,29] The inhibitory DAD-DID interaction is mediated by 'core' MDxLLExL and 'basic' RRKR motifs in the DAD (**Fig. 2**) that bind cognate DID sequences.[30]

Reverse-transcriptase (RT) PCR and PCR amplification of the R1213 region and subsequent restriction endonuclease digestion proved the presence of both wild type and R1213* DIAPH1 mRNA transcripts in platelets from cases 10 and 16 (**Supplementary Fig. 2**). The premature stop codon created by the R1213* variant occurs at position 1 of the RRKR motif (residues 1213-1216), but is closer to the DIAPH1 carboxyl terminus than the MDxLLExL motif (residues 1199-1206). Therefore, the predicted consequence of the R1213* variant is expression of

DIAPH1 protein with a truncation within the DAD resulting in loss of the RRKR motif, but not the MDxLLExL motif (**Fig. 2**).

DIAPH1 R1213* is associated with syndromic MTP and hearing loss.

All eight genotyped R1213* cases had thrombocytopenia (baseline automated platelet counts 63-147 $x10^9$ L^{-1}) and enlarged platelets (mean platelet volume (MPV) 11.2-14.1 fL), confirmed by light microscopy (**Fig 3a.** and **Table 1**) and by morphometric analysis of platelet electron micrographs (**table 2**). The platelet count ranges in the male and female cases corresponded to the 0.15-2.81th percentiles and 0.08-0.38th percentiles respectively of a sex-stratified population of 443,142 UK BioBank volunteers. For MPV, the corresponding percentiles were 99.81-99.83 and 94.14-99.92 (**Supplementary Fig.3**). Asymptomatic mild neutropenia was observed on at least one occasion in six cases (range of neutrophil counts 0.62-4.34 $x10^9$ L^{-1}), but varied within the cases at different times (**Table 1**). The erythroid lineage was normal in all the cases. Platelets from three tested cases showed normal aggregation with ADP (2.5-10 µM), collagen (2 µg mL^{-1}), arachidonic acid (0.5 mg mL^{-1}), TRAP-14mer (50 µM) and ristocetin (0.5-1-5 mg mL^{-1}). ADP and TRAP-stimulated dense granule secretion determined by measuring ATP release (cases 10, 16, 17 and 21) and α-granule secretion (cases 10 and 16) determined by measuring P-selectin surface exposure, were unchanged compared to controls. Platelet surface expression of $\alpha_{IIb}\beta3$ integrin and glycoprotein Ib-IX-V (cases 10, 16 and 17) was slightly increased compared with controls, consistent with the increased platelet size. Electron microscopy (cases 10, 16, 17 and 21) showed that the enlarged platelets were typically round, although occasionally highly elongated. There were also abnormal

vacuoles, membrane complexes and abnormally distributed α-granules, some of which were unusually large (**Fig. 3b**).

Abnormal bleeding symptoms comprised menorrhagia and mild subcutaneous bleeding in case 17 and a post-partum bleed in case 21, but were absent in the other cases. The sensorineural hearing loss that segregated with MTP was detected either at birth or in the first decade of life but progressed rapidly to a severe defect requiring bilateral hearing aids in all eight cases.

Abnormal maturation of DIAPH1 R1213* MK.

Assessment of MK proliferation, differentiation and proplatelet formation of $CD34^+$ stem cell-derived MKs from case 21 and controls on two separate occasions, revealed similar numbers of MK colony forming units (CFU-MK) at day 12 of culture (**Fig. 4a**). However, the MK colonies from case 21 had a higher cell density compared to controls (**Fig. 4b** and **Supplementary Fig. 4**). Suspension cultures from case 21 showed a pronounced defect in PPF compared to controls in two independent experiments (**Fig. 4c** and **4d**). In addition, we found numerous MK clusters containing small and large MKs (**Fig. 4d** and **Supplementary Fig. 5**) in cultures from case 21, that were not present in control cultures, which hampered analysis of MK ploidy by flow cytometry (**Supplementary Fig. 6**).

Confocal microscopy of control MKs on day 12 of culture showed a partial co-localization of CD61 and filamentous actin (F-actin), which was not observed in MKs from case 21 (**Fig. 4e**). There was also aberrant architecture of the cortical F-actin cytoskeleton in MKs from case 21 and small filopodia-like protrusions and F-actin

positive junctions at the contact zones of clustered MKs (**Fig. 4e**). This is in line with previous studies where DIAPH1 was shown to regulate adherens junctions via the actin network.[31, 32]

The R1213* variant is associated with altered DIAPH expression in platelets.

We next investigated the effect of the R1213* variant on DIAPH1 expression in platelets by performing Western blots using an antibody recognising the DIAPH1 amino-terminus. In platelets from cases 10, 16, and 21, the 155 kDa band, corresponding to full length DIAPH1 protein, was decreased in intensity compared with controls, while a band of approximately 80 kDa was more intense (**Fig. 5a**; **Supplementary Fig. 7**). The 80 kDa band did not correspond to any *DIAPH1* transcripts listed in Ensembl, but following immunoprecipitation and mass-spectrometry, was found to contain peptide sequences with 57% coverage across the full length of the DIAPH1 protein sequence (**Supplementary information**). Moreover, this band was also immunoreactive with antibodies recognising the DIAPH1 carboxyl terminus, suggesting that it resulted from limited proteolysis of DIAPH1 in platelets. Since DIAPH1 expressed from the R1213* variant allele is predicted to have only a 60 amino acid truncation, it was not possible to resolve the relative contribution of the variant DIAPH1 to either of the immunoreactive bands.

Western blots generated from platelets from the R1213* cases also showed increased DIAPH2 and DIAPH3 expression compared with controls (**Fig. 5a**). Expression of DIAPH2 and DIAPH3 has previously been observed to decrease during MK maturation,[17] which we confirmed by RNA-seq analysis (**Supplementary Fig. 8**). Therefore, our observations in the R1213* cases are consistent with platelet

formation from MK with deregulated maturation and support the previous observations in MK from bone marrow and culture (**Fig. 4a** and **4b**).[17]

DIAPH1 R1213* and altered platelet cytoskeleton.

Using confocal microscopy, we found that DIAPH1 was localised to the peripheral marginal band in resting platelets from controls, but was distributed throughout the cytoplasm of platelets from the R1213* cases 10 and 16 (**Fig. 5b**). There was also increased F-actin and α-tubulin staining, and aberrant organisation of microtubules compared with controls (**Fig. 5b**). Electron microscopy confirmed microtubule disorganisation (**Fig. 5c**) and quantification by manual counting revealed approximately 2.6 fold more microtubule coils in platelets from the R1213* cases compared to controls (**Fig. 5d**). Incubation of platelets from controls at 4°C caused disassembly of microtubules, which then reassembled to the marginal band after rewarming to 37°C, as previously reported.[22-24] In contrast, cold incubation or rewarming did not grossly affect the microtubules in platelets from the R1213* cases (**Fig. 6a**), suggesting that the increased microtubule content resulted from increased microtubule stability.

The formation of stable microtubules is associated with post-translational detyrosination (Glu-tub) and acetylation (ac-tub) of α-tubulin, whereas dynamic microtubules are characterised by unmodified tyrosinated α-tubulin (Tyr-tub).[33,34] Following treatment with colchicine or cold incubation to destabilise microtubules, platelets from the R1213* cases 10 and 16 showed a higher content of stable detyrosinated and acetylated microtubules, compared with controls (**Fig. 6b**; **Supplementary Fig. 9** and **10**). During spreading on fibrinogen, platelets from the

R1213* cases maintained detyrosinated and acetylated microtubules, whereas these modifications were not detected in controls (**Fig. 6c**). Platelets from the R1213* cases also displayed an increased content and aberrant organization of F-actin, particularly at the platelet cortex where there was increased formation of small filopods (**Fig. 6c**). Fractionation of the tubulin cytoskeleton by ultracentrifugation revealed higher ac-tub/Tyr-tub and Glu-tub/Tyr-tub band density ratios in the R1213* cases compared with controls, particularly in the polymerised (pellet) microtubule fraction, confirming a higher content of stable microtubules (**Fig. 6d** and **Supplementary Fig. 10**).

DIAPH1 R1213* alters cytoskeletal organisation in cell lines.

In HEK293FT cells transfected with wild type (DIAPH1 WT) or variant (DIAPH1 R1213*) expression constructs, Western blots confirmed overexpression of both DIAPH1 WT and DIAPH1 R1213* proteins. However, in contrast to platelets from the R1213* cases, expression of DIAPH2 or DIAPH3 was not increased, allowing us to study the effect of the truncated R1213* DIAPH1 variant in isolation (**Fig. 7a**). Transfection of the human adenocarcinoma lung (A549) epithelial cell line with both expression constructs increased the prevalence of F-actin and acetylated and detyrosinated microtubules compared with adjacent untransfected cells. This effect was more pronounced in DIAPH1 R1213* (**Fig. 7b** and **7c**) than in DIAPH1 WT cells (**Supplementary Fig. 11**).

Western blot analysis of microtubule fractions showed that the DIAPH1 R1213* transfected HEK293FT cells had a higher content of acetylated and detyrosinated microtubules in the polymerised tubulin fraction, compared with DIAPH1 WT or

mock-transfected controls (**Fig. 7e** and **Supplementary Fig. 11**), thereby reproducing the cytoskeletal alterations found in platelets from the cases. Incubation of the cells with the small molecule FH2-domain inhibitor SMIFH2 did not influence expression of DIAPH1, 2 or 3 (**Fig. 7a**) and did not prevent stabilisation of microtubules by DIAPH1 R1213* (**Fig. 7d** and **7e**). However, SMIFH2 did prevent the increase in F-actin content in cells overexpressing DIAPH1 R1213* (**Fig. 7d**) confirming that the DIAPH1 FH2 domain is critical for the F-actin polymerisation.

DISCUSSION

We have identified *DIAPH1* as a novel candidate gene for dominant MTP and sensorineural hearing loss by analysis of the largest ever assembled collection of cases with previously uncharacterised BPD. Essential to this discovery was the annotation of the characteristics of the cases with HPO terms for haematological features and phenotypes in other organ systems, and then statistical analysis to identify similarities in HPO terms between cases. We have previously shown that cluster analysis of HPO terms within a large BPD case collection enabled identification of causal variants in *ACTN1* and *MYH9* that have previously been associated with MTP.[7, 9] However, the statistical evidence supporting *DIAPH1* as a candidate gene could only be obtained by applying a novel similarity regression method to the phenotype and genotype data.[19] Specifically, similarity regression revealed a hitherto unidentified association between a characteristic phenotype that was ontologically similar for two unrelated index cases and the shared presence of a high impact variant in *DIAPH1.* We also showed that the high impact variant in *DIAPH1* was the same premature stop variant R1213* in both index cases and that this segregated with MTP

and sensorineural hearing loss in a further six pedigree members, thereby confirming linkage with R1213*.

It is noteworthy that *DIAPH1* has been identified previously as the candidate gene for non-syndromic sensorineural deafness type DFNA1 (ORPHA90635) in a single characterised pedigree, in which hearing loss typically developed later in childhood than in the R1213* cases.[35, 36] The causal variant for DFNA1 caused aberrant splicing of *DIAPH1* in lymphocyte cDNA that predicted expression of DIAPH1 with an abnormal carboxyl terminus sequence from glutamine 1220, and chain truncation after a further 21 amino acids.[35] No platelet count or volume data are reported for the DFNA1 pedigree preventing a direct comparison with the R1213* pedigrees reported here. However, an important difference is that the DFNA1 variant disrupts only the two final residues in the DIAPH1 DAD domain (1194-1222 in UNIPROT O60610). In contrast to R1213*, this does not result in loss of the autoregulatory basic RRKR motif. Absent expression of DIAPH1 resulting from a homozygous stop-gain variant at codon 778 has been associated previously with a distinct disorder of short stature, microcephaly and visual impairment without reported hearing or haematological phenotypes.[37]

MTP and hearing loss may also co-segregate in MYH9-related disorder (MYH9-RD; ORPHA182050) in which abnormal expression of non-muscle myosin heavy chain IIa alters myosin-dependent organelle distribution and F-actin organisation, thereby disrupting MK proplatelet formation.[13, 14] Aberrant cytoskeletal organisation in inner ear stereocilia has been proposed as a mechanism for hearing loss in MYH9-RD,[16] and may contribute to this phenotype in the DIAPH1 R1213* cases. However, there

are also several characteristics of the DIAPH1 R1213* cases that are absent in MYH9-RD. For example, platelets in the R1213* cases were elongated or round, moderately enlarged and contained few membrane complexes, whereas in MYH9-RD, platelets are highly enlarged and contain abundant membrane complexes. Hearing loss was early onset and severe in the R1213* cases but develops in only 35% of MYH9-RD cases, typically after 10 years of age.[10] Cataract and nephropathy are reported in 5% and 21% of MYH9-RD cases respectively,[10] but were absent in the R1213* cases.

DIAPH1 is a conserved member of the formin protein family, which mediate Rho-GTPase dependent assembly of F-actin and microtubule regulation during cytoskeletal remodelling in cytokinesis, organelle trafficking and filopodia formation. Several mammalian formins mediate cell differentiation and adhesive events required for haematopoiesis.[25, 38] However, a critical negative regulatory role for DIAPH1 is indicated by observations that targeted knockout of the murine *DIAPH1* ortholog *Drf1* resulted in hyperproliferative myelodysplasia.[39, 40] Consistent with this, DIAPH1 knockdown in cultured human MK, resulted in increased proplatelet formation.[17] In contrast, overexpression of a constitutively active DIAPH1 in which both the DID and DAD were deleted by artificial mutagenesis (mDiaΔN3), reduced proplatelet formation in cultured human MK. [17] We also observed reduced proplatelet formation in $CD34^+$ cell-derived MK from R1213* case 21, suggesting that this variant may also result in constitutive activation of DIAPH1. The MK culture experiments also suggested that the R1213* variant was associated with enhanced MK proliferation as an increased number of cells was present in the separate CFU-MK colonies from case 21. As a consequence of the increased cell density in the

CFU-MK colonies, we were unable to confirm this by counting the total number of single MKs. However, ploidy analysis of suspension cultures revealed no obvious differences in MK endomitosis as both large and small MKs were present in cultures from case 21. Further studies are required to evaluate the possibility of a hyperproliferative effect of early MKs due to the R1213* variant.

The hypothesis that the R1213* variant results in constitutively active DIAPH1 is also supported by the prediction that R1213* results in partial truncation of the autoregulatory DIAPH1 DAD. Mutagenesis of the DAD has been shown previously to increase the formation of stable microtubule networks and F-actin bundles in cell models,[41, 42] consistent with loss of the inhibitory DID-interaction. This interaction is mediated in part by a DAD core MDxLLExL motif, which is unaffected by the R1213* variant. However, there is also an inhibitory interaction between the DAD basic RRKR motif that is absent in the R1213* variant, and a cognate acidic groove in the DID.[30] This second site of DID-DAD interaction is necessary for complete auto-regulation of DIAPH1 since selective mutagenesis of the basic RRKR motif also conferred constitutive activity to DIAPH1 orthologs, resulting in abnormal F-actin polymerisation and altered cell architecture.[42, 43]

We provided experimental support for constitutive activation of DIAPH1 by showing disorganisation of actin filaments and increased stability and content of microtubules in platelets from the R1213* cases (**Fig. 6a-d**). Overexpression of DIAPH1 R1213* also resulted in increased assembly of actin filaments and stabilisation of microtubules in cell lines (**Fig. 7**), thereby reproducing the cytoskeletal alterations observed in platelets from the R1213* cases. These effects on cytoskeletal organisation may

account directly for the reduced proplatelet formation from MKs derived from the cases (**Fig. 4c** and **4d**), since highly regulated microtubule and F-actin dynamics are necessary for proplatelet extension and branching.[4, 44, 45] It is noteworthy that overexpression of the constitutively active DIAPH1 mDiaΔN3 which reduced proplatelet formation in cultured human MK, was shown previously to increase polymerisation of filamentous actin, similar to that observed with the R1213* variant. However, in MKs overexpressing mDiaΔN3, microtubule stability was reduced showing that the cytoskeletal alterations do not completely reproduce those associated with the R1213* variant.[17] One possible explanation for this difference is that in contrast to R1213*, the mDiaΔN3 model additionally carries an N-terminal deletion including the Rho GTPase-binding domain of DIAPH1, potentially causing a different effect of DIAPH1 regulation.[17, 42]

The gain-of-function R1213* *DIAPH1* variant represents a new human dominant syndromic disorder of MTP and sensorineural hearing loss that is clinically distinct from other MTP disorders and has different characteristics than *DIAPH1* gene deletion models. The platelet phenotype of the R1213* variant cases highlights the impact of abnormal regulation of DIAPH1 on cytoskeletal organisation during platelet production.

ACKNOWLEDGEMENTS

This research has been conducted by using full blood count data from the UK Biobank Resource. We would like to thank Xavier Pillois and Line Pourtau from the Institut Hospitalo-Universitaire LIRYC, Pessac in France for their help in the preparation of DNA samples and of platelet samples, respectively. We acknowledge

Dr Stephanie Burger-Stritt for assistance with blood withdrawals, Dr Stephanie Lamer and Professor Andreas Schlosser for their assistance with mass spectrometry and the microscopy platform of the Rudolf Virchow Centre. The authors wish also to express their gratitude to many colleagues and their patients who have made the BRIDGE Bleeding and Platelets Disorders study possible.

FUNDING ACKNOWLEDGEMENTS

The NIHR BioResource- Rare Diseases and the associated BRIDGE genome sequencing projects are supported by the National Institute for Health Research (NIHR; http://www.nihr.ac.uk, award number RG65966). B.N. was supported by the Deutsche Forschungsgemeinschaft (SFB 688). S.S. was supported by a grant of the German Excellence Initiative to the Graduate School of Life Sciences, University of Würzburg. ET, DG, JCS, SP, IS, CJP, RM, SAsh, ST and KS are supported by the NIHR BioResource - Rare Diseases. KF, CT, and CVG are supported by the Fund for Scientific Research-Flanders (FWO-Vlaanderen, Belgium, G.0B17.13N) and by the Research Council of the University of Leuven (BOF KU Leuven, Belgium, OT/14/098). WNE is supported by the Cancer Council Western Australia. Research in the Ouwehand laboratory is supported by program grants from the European Commission and NIHR to WJA, SM, MK, RP, SBJ and WHO under award numbers RG65309 and RG59534; the laboratory also receives funding from NHS Blood and Transplant; CL and SKW are supported by Medical Research Council (MRC) Clinical Training Fellowships (number MR/K023489/1) and TKB by a British Society of Haematology/NHS Blood and Transplant grant. MAL and CL are supported by the Imperial College London Biomedical Research Centre; JRB acknowledges support by the NIHR Cambridge Biomedical Research Centre and SR

by the Medical Research Council and Cambridge Biomedical Research Centre. CVG is holder of the Bayer and Norbert Heimburger (CSL Behring) Chairs. ADM is supported by the NIHR Bristol Cardiovascular Biomedical Research Unit.

AUTHOR CONTRIBUTIONS

PN initiated the collaboration of the French Reference Center on Inherited Platelet Disorders and established the joint working with the BRIDGE-BPD consortium. She enrolled cases, designed and performed experiments and co-wrote the paper with SS, ET, DG, KF, BN, AN, WHO and ADM. SMar provided expert advice on the observed hearing disorder in the cases. SS designed and performed experiments and was supervised by AN, BN and PN. ADM enrolled cases, collected phenotype data and with KF, designed and oversaw experiments by SKW and CT. WNE reviewed blood films and provided expert bone marrow pathology interpretation. WHO and FLR direct the NIHR BioResource- Rare Diseases and oversees with KS the DNA handling (JCS, RM) and genome sequencing (analysis by CJP and ST), whole exome sequencing (by IS) and Illumina Cambridge Ltd (whole genome sequencing). SAsh provided ethics support and NIHR BioResource – Rare Diseases study management. JRB established and directs the NIHR BioResource, a collaborative network for enrolment across England. WHO established and directs with MAL and CVG the BRIDGE-BPD consortium and directs with SR the genetic analysis by ET (chief analyst) and DG, who developed the similarity regression model and assisted with analysis and manuscript preparation. WJA analysed the full blood count data from the UK BioBank cohort. SBJ performed the experiments underlying the sequencing of RNA from immature (CD42b negative) and mature (CD42b positive) megakaryocytes (MKs) and RNA-seq data were analyzed by RP,

who was supervised by MK. SMai performed experiments on the *DIAPH1* transcripts. SKW, CL, TKB, AMK, TB, PC, RF, MPL, MM, CMM, KP, DJP, SS, other members of the BRIDGE-BPD Consortium, KG, PN and CVG enrolled cases and collected phenotype data. JCS encoded the pedigrees. SP was the study co-ordinator, provided ethics support and assisted with manuscript preparation.

DISCLOSURE OF CONFLICTS OF INTEREST

The authors have declared that there are no relevant conflicts of interest.

REFERENCES

1. Patel SR, Hartwig JH and Italiano JE, Jr. The biogenesis of platelets from megakaryocyte proplatelets. *J Clin Invest*. 2005;115:3348-54.

2. Bluteau D, Lordier L, Di Stefano A, Chang Y, Raslova H, Debili N and Vainchenker W. Regulation of megakaryocyte maturation and platelet formation. *J Thromb Haemost*. 2009;7 Suppl 1:227-34.

3. Junt T, Schulze H, Chen Z, Massberg S, Goerge T, Krueger A, Wagner DD, Graf T, Italiano JE, Jr., Shivdasani RA and von Andrian UH. Dynamic visualization of thrombopoiesis within bone marrow. *Science*. 2007;317:1767-70.

4. Italiano JE, Jr., Lecine P, Shivdasani RA and Hartwig JH. Blood platelets are assembled principally at the ends of proplatelet processes produced by differentiated megakaryocytes. *J Cell Biol.* 1999;147:1299-312.

5. Pecci A and Balduini CL. Lessons in platelet production from inherited thrombocytopenias. *Br J Haem*. 2014;165:179-92.

6. Noris P, Biino G, Pecci A, Civaschi E, Savoia A, Seri M, Melazzini F, Loffredo G, Russo G, Bozzi V, Notarangelo LD, Gresele P, Heller PG, Pujol-Moix N,

Kunishima S, Cattaneo M, Bussel J, De Candia E, Cagioni C, Ramenghi U, Barozzi S, Fabris F and Balduini CL. Platelet diameters in inherited thrombocytopenias: analysis of 376 patients with all known disorders. *Blood*. 2014;124:e4-e10.

7. Kunishima S, Okuno Y, Yoshida K, Shiraishi Y, Sanada M, Muramatsu H, Chiba K, Tanaka H, Miyazaki K, Sakai M, Ohtake M, Kobayashi R, Iguchi A, Niimi G, Otsu M, Takahashi Y, Miyano S, Saito H, Kojima S and Ogawa S. ACTN1 mutations cause congenital macrothrombocytopenia. *Am J Hum Genet.* 2013;92:431-8.

8. Nurden P, Debili N, Coupry I, Bryckaert M, Youlyouz-Marfak I, Sole G, Pons AC, Berrou E, Adam F, Kauskot A, Lamaziere JM, Rameau P, Fergelot P, Rooryck C, Cailley D, Arveiler B, Lacombe D, Vainchenker W, Nurden A and Goizet C. Thrombocytopenia resulting from mutations in filamin A can be expressed as an isolated syndrome. *Blood*. 2011;118:5928-37.

9. Pecci A, Klersy C, Gresele P, Lee KJ, De Rocco D, Bozzi V, Russo G, Heller PG, Loffredo G, Ballmaier M, Fabris F, Beggiato E, Kahr WH, Pujol-Moix N, Platokouki H, Van Geet C, Noris P, Yerram P, Hermans C, Gerber B, Economou M, De Groot M, Zieger B, De Candia E, Fraticelli V, Kersseboom R, Piccoli GB, Zimmermann S, Fierro T, Glembotsky AC, Vianello F, Zaninetti C, Nicchia E, Guthner C, Baronci C, Seri M, Knight PJ, Balduini CL and Savoia A. MYH9-related disease: a novel prognostic model to predict the clinical evolution of the disease based on genotype-phenotype correlations. *Hum mutat*. 2014;35:236-47.

10. Saposnik B, Binard S, Fenneteau O, Nurden A, Nurden P, Hurtaud-Roux MF, Schlegel N and French MYHn. Mutation spectrum and genotype-phenotype correlations in a large French cohort of MYH9-Related Disorders. *Mol Genet Genomic Med.* 2014;2:297-312.

11. Kunishima S, Kobayashi R, Itoh TJ, Hamaguchi M and Saito H. Mutation of the beta1-tubulin gene associated with congenital macrothrombocytopenia affecting microtubule assembly. *Blood*. 2009;113:458-61.

12. Manchev VT, Hilpert M, Berrou E, Elaib Z, Aouba A, Boukour S, Souquere S, Pierron G, Rameau P, Andrews R, Lanza F, Bobe R, Vainchenker W, Rosa JP, Bryckaert M, Debili N, Favier R and Raslova H. A new form of macrothrombocytopenia induced by a germ-line mutation in the PRKACG gene. *Blood*. 2014;124:2554-63.

13. Pertuy F, Eckly A, Weber J, Proamer F, Rinckel JY, Lanza F, Gachet C and Leon C. Myosin IIA is critical for organelle distribution and F-actin organization in megakaryocytes and platelets. *Blood*. 2014;123:1261-9.

14. Chen Y, Boukour S, Milloud R, Favier R, Saposnik B, Schlegel N, Nurden A, Raslova H, Vainchenker W, Balland M, Nurden P and Debili N. The abnormal proplatelet formation in MYH9-related macrothrombocytopenia results from an increased actomyosin contractility and is rescued by myosin IIA inhibition. *J Thromb Haemost.* 2013;11:2163-75.

15. Kunishima S, Nishimura S, Suzuki H, Imaizumi M and Saito H. TUBB1 mutation disrupting microtubule assembly impairs proplatelet formation and results in congenital macrothrombocytopenia. *Eur J Haem*. 2014;92:276-82.

16. Balduini CL, Pecci A and Savoia A. Recent advances in the understanding and management of MYH9-related inherited thrombocytopenias. *Br J Haem*. 2011;154:161-74.

17. Pan J, Lordier L, Meyran D, Rameau P, Lecluse Y, Kitchen-Goosen S, Badirou I, Mokrani H, Narumiya S, Alberts AS, Vainchenker W and Chang Y. The

formin DIAPH1 (mDia1) regulates megakaryocyte proplatelet formation by remodeling the actin and microtubule cytoskeletons. *Blood*. 2014;124:3967-77.

18. Westbury SK, Turro E, Greene D, Lentaigne C, Kelly AM, Bariana TK, Simeoni I, Pillois X, Attwood A, Austin S, Jansen SB, Bakchoul T, Crisp-Hihn A, Erber WN, Favier R, Foad N, Gattens M, Jolley JD, Liesner R, Meacham S, Millar CM, Nurden AT, Peerlinck K, Perry DJ, Poudel P, Schulman S, Schulze H, Stephens JC, Furie B, Robinson PN, van Geet C, Rendon A, Gomez K, Laffan MA, Lambert MP, Nurden P, Ouwehand WH, Richardson S, Mumford AD, Freson K and Consortium B-B. Human phenotype ontology annotation and cluster analysis to unravel genetic defects in 707 cases with unexplained bleeding and platelet disorders. *Genome medicine*. 2015;7:36.

19. Greene D. BC, Ouwehand, W.H.O. Sylvia Richardson, S., Turro,E. Phenotype similarity regression for rare disease gene discovery. *Am J Hum Gen* 2015 (manuscript under review)

20. Louwette S, Regal L, Wittevrongel C, Thys C, Vandeweeghde G, Decuyper E, Leemans P, De Vos R, Van Geet C, Jaeken J and Freson K. NPC1 defect results in abnormal platelet formation and function: studies in Niemann-Pick disease type C1 patients and zebrafish. *Hum mol genet*. 2013;22:61-73.

21. Freson K, Peeters K, De Vos R, Wittevrongel C, Thys C, Hoylaerts MF, Vermylen J and Van Geet C. PACAP and its receptor VPAC1 regulate megakaryocyte maturation: therapeutic implications. *Blood*. 2008;111:1885-93.

22. Bender M, Stritt S, Nurden P, van Eeuwijk JM, Zieger B, Kentouche K, Schulze H, Morbach H, Stegner D, Heinze KG, Dutting S, Gupta S, Witke W, Falet H, Fischer A, Hartwig JH and Nieswandt B. Megakaryocyte-specific Profilin1-

deficiency alters microtubule stability and causes a Wiskott-Aldrich syndrome-like platelet defect. *Nat Comm*. 2014;5:4746.

23. Meyer I, Kunert S, Schwiebert S, Hagedorn I, Italiano JE, Jr., Dutting S, Nieswandt B, Bachmann S and Schulze H. Altered microtubule equilibrium and impaired thrombus stability in mice lacking RanBP10. *Blood*. 2012;120:3594-602.

24. Schulze H, Korpal M, Hurov J, Kim SW, Zhang J, Cantley LC, Graf T and Shivdasani RA. Characterization of the megakaryocyte demarcation membrane system and its role in thrombopoiesis. *Blood*. 2006;107:3868-75.

25. Chesarone MA, DuPage AG and Goode BL. Unleashing formins to remodel the actin and microtubule cytoskeletons. *Nat Rev Mol Cell Biol*. 2010;11:62-74.

26. Goode BL and Eck MJ. Mechanism and function of formins in the control of actin assembly. *Ann Rev Biochem*. 2007;76:593-627.

27. Maiti S, Michelot A, Gould C, Blanchoin L, Sokolova O and Goode BL. Structure and activity of full-length formin mDia1. *Cytoskeleton*. 2012;69:393-405.

28. Rose R, Weyand M, Lammers M, Ishizaki T, Ahmadian MR and Wittinghofer A. Structural and mechanistic insights into the interaction between Rho and mammalian Dia. *Nature*. 2005;435:513-8.

29. Otomo T, Otomo C, Tomchick DR, Machius M and Rosen MK. Structural basis of Rho GTPase-mediated activation of the formin mDia1. *Mol Cell*. 2005;18:273-81.

30. Nezami A, Poy F, Toms A, Zheng W and Eck MJ. Crystal structure of a complex between amino and carboxy terminal fragments of mDia1: insights into autoinhibition of diaphanous-related formins. *PloS one*. 2010;5.

31. Sahai E and Marshall CJ. ROCK and Dia have opposing effects on adherens junctions downstream of Rho. *Nat Cell Biol*. 2002;4:408-15.

32. Carramusa L, Ballestrem C, Zilberman Y and Bershadsky AD. Mammalian diaphanous-related formin Dia1 controls the organization of E-cadherin-mediated cell-cell junctions. *J Cell Sci*. 2007;120:3870-82.

33. Gundersen GG, Kalnoski MH and Bulinski JC. Distinct populations of microtubules: tyrosinated and nontyrosinated alpha tubulin are distributed differently in vivo. *Cell*. 1984;38:779-89.

34. Webster DR and Borisy GG. Microtubules are acetylated in domains that turn over slowly. *J Cell Sci*. 1989;92 (Pt 1):57-65.

35. Lynch ED, Lee MK, Morrow JE, Welcsh PL, Leon PE and King MC. Nonsyndromic deafness DFNA1 associated with mutation of a human homolog of the Drosophila gene diaphanous. *Science*. 1997;278:1315-8.

36. Leon PE, Bonilla JA, Sanchez JR, Vanegas R, Villalobos M, Torres L, Leon F, Howell AL and Rodriguez JA. Low frequency hereditary deafness in man with childhood onset. *AmJ Hum Genet.* 1981;33:209-14.

37. Ercan-Sencicek AG, Jambi S, Franjic D, Nishimura S, Li M, El-Fishawy P, Morgan TM, Sanders SJ, Bilguvar K, Suri M, Johnson MH, Gupta AR, Yuksel Z, Mane S, Grigorenko E, Picciotto M, Alberts AS, Gunel M, Sestan N and State MW. Homozygous loss of DIAPH1 is a novel cause of microcephaly in humans. *Eur J Hum Genet*. 2015;23:165-72.

38. Ji P, Jayapal SR and Lodish HF. Enucleation of cultured mouse fetal erythroblasts requires Rac GTPases and mDia2. *Nat Cell Biol.* 2008;10:314-21.

39. Peng J, Kitchen SM, West RA, Sigler R, Eisenmann KM and Alberts AS. Myeloproliferative defects following targeting of the Drf1 gene encoding the mammalian diaphanous related formin mDia1. *Cancer research*. 2007;67:7565-71.

40. Keerthivasan G, Mei Y, Zhao B, Zhang L, Harris CE, Gao J, Basiorka AA, Schipma MJ, McElherne J, Yang J, Verma AK, Pellagatti A, Boultwood J, List AF, Williams DA and Ji P. Aberrant overexpression of CD14 on granulocytes sensitizes the innate immune response in mDia1 heterozygous del(5q) MDS. *Blood*. 2014;124:780-90.

41. Ishizaki T, Morishima Y, Okamoto M, Furuyashiki T, Kato T and Narumiya S. Coordination of microtubules and the actin cytoskeleton by the Rho effector mDia1. *Nat Cell Biol*. 2001;3:8-14.

42. Watanabe N, Kato T, Fujita A, Ishizaki T and Narumiya S. Cooperation between mDia1 and ROCK in Rho-induced actin reorganization. *Nat Cell Biol*. 1999;1:136-43.

43. Wallar BJ, Stropich BN, Schoenherr JA, Holman HA, Kitchen SM and Alberts AS. The basic region of the diaphanous-autoregulatory domain (DAD) is required for autoregulatory interactions with the diaphanous-related formin inhibitory domain. *J Biol Chem*. 2006;281:4300-7.

44. Tablin F, Castro M and Leven RM. Blood platelet formation in vitro. The role of the cytoskeleton in megakaryocyte fragmentation. *J Cell Sci*. 1990;97 (Pt 1):59-70.

45. Patel-Hett S, Richardson JL, Schulze H, Drabek K, Isaac NA, Hoffmeister K, Shivdasani RA, Bulinski JC, Galjart N, Hartwig JH and Italiano JE, Jr. Visualization of microtubule growth in living platelets reveals a dynamic marginal band with multiple microtubules. *Blood*. 2008;111:4605-16.

FIGURE LEGENDS

Figure 1: *DIAPH1* is a candidate gene for macrothrombocytopenia and hearing loss (**a**) Each BPD index case was coded using Human Phenotype Ontology (HPO) terms relating to haematological features and to phenotypes in other organ systems and underwent high throughput sequencing.[18] Candidate genes for BPD were identified by similarity regression in which 'baseline' and 'alternate' statistical models are compared for every gene.[19] Under the baseline model, all cases are assumed to have the same log odds of carrying a rare variant. Under the alternate model, which we give a prior probability of 0.05 of being the true model, the log odds is modelled as a linear function of the phenotypic similarity of each case to an HPO-encoded "characteristic phenotype". The characteristic phenotype (φ) and a binary variable indicating the true model (γ) are inferred from the genotype and phenotype data. A high posterior mean for γ is indicative of a potential association between the presence of a rare variant in a gene and a disorder characterised by φ. The histogram indicates the mean posterior probability of the alternate model being true for all 1,073 genes in which at least two BPD cases carry a high-impact variant. The value for *DIAPH1* is indicated in red. (**b**) The inferred HPO-coded characteristic phenotype (φ) for *DIAPH1* is represented as a graph. Each edge denotes an *is-a* relationship and each node contains an abbreviated HPO term with its marginal posterior probability of inclusion in φ, which is also represented by the node size. If a node and all its descendants in the HPO graph have a marginal posterior probability of inclusion in φ less than 0.02, it is not shown (BBFT: Abnormality of blood and blood forming tissues; TCP: Thrombocytopenia; FAIE: Functional abnormality of the inner ear; SNHI: Sensorineural hearing impairment. Some terms have been shortened for conciseness). (**c**) Pedigrees of the index cases (*) in which the coloured symbols

indicate macrothrombocytopenia (black) and hearing loss (red). The grey symbols indicate that the clinical phenotype is unknown and the white symbols indicate no macrothrombocytopenia or hearing loss. Genotyped cases are indicated by +/M for the heterozygous *DIAPH1* R1213* variant and +/+ for the reference sequence at that locus.

Figure 2: Location of the DIAPH1 R1213* variant:

Schematic representation of the major MK *DIAPH1* transcript ENST00000398557 which is predicted to encode the 1272 amino acid DIAPH1 protein. R1213 is 60 amino acids from the carboxyl terminus of DIAPH1 within the diaphanous autoregulatory domain (DAD). In the amino acid sequence line up of human DIAPH1 and orthologues, there is conservation of the core MDxLLExL (blue box) and basic RRKR (green box) motifs within the DAD that mediate auto-inhibitory interactions with the diaphanous inhibitory domain (DID) near the amino terminus of DIAPH1. Since R1213 is at position 1 of the basic RRKR motif, R1213* is predicted to cause expression of a truncated DIAPH1 protein with an intact core MDxLLExL motif, but without the basic RRKR motif.

Figure 3: Effect of R1213* variant on platelet morphology:

Illustration of the typical platelet morphology for cases 10, 16, 17, 21 on a May-Grünwald-Giemsa (MGG) stained blood smear for case 21 (**A**) and by TEM (**B**). Plaetlets of control (C) are discoid, of regular size with homogeneously distributed granules. All examined platelets of the patients show a heterogeneous size, shape, and distribution of α-granules. (**A**) Arrows highlight platelets (case 21) of different size colored by MGG. (**B**) TEM revealed an abnormal large granule (LG). In the

middle panel a very thin elongated platelet can be seen, other platelets with a more round shape have few granules. In the lower panel a very round platelet with many granules is illustrated (case 17) the other platelets from case 16 show an abnormal presence of vacuoles (V) and a membrane complex (MC) case 17. Scale bars, 1 µm. The TEM images were acquired using either an EM900 (Carl Zeiss) or a JEM-1010 (JEOL) transmission electron microscope.

Figure 4: Repeated megakaryocyte proliferation, differentiation and proplatelet-formation studies for a R1213* variant case: (**a**) Total amount of CFU-MK colonies derived from peripheral blood $CD34^+$ mononuclear cells from a control (C) and case 21 (21) at day 12 of culture. This experiment was repeated at two independent occasions (Exp 1 and Exp 2). (**b**) Representative images of cultured CFU-MK colonies from a control (C) and case 21 (21) at day 12 of culture visualised by light microscopy after staining with May-Grünwald-Giemsa (Exp 2). Scale bars, 50 µm. (**c**) MK in suspension triplicated liquid cultures performed at two independent occasions were classified as proplatelet forming (PPF-MK) if proplatelet extensions were visible by light microscopy. The proportion of PPF-MK was lower in the cultures from case 21 compared to controls (One way Anova; ***P>0.001). (**d**) Representative light microscopy images of cultured MK showing formation of proplatelet extensions for the control. PPF MKs are almost absent for the case 21 while they typically present in MK clusters that contain large and small cells. Scale bars, 20 µm. (**e**) Immunofluorescence confocal microcopy images of differentiated fibrinogen-adhered MK at day 12 of culture visualised by anti-integrin β3 (green, CD61) and phalloidin (red, F-actin) staining, showing co-localisation in MKs from

control but not from case 21. Scale bars 20 μm. Numerous PPF MKs are present in the control (representative image) while MKs for case 21 form clusters.

Figure 5: Altered expression of DIAPH1-3 and cytoskeletal organisation in platelets from R1213* variant cases: (**a**) Representative Western blots of resolved platelet protein extracts from R1213* cases (10 and 16) and from control (C), probed with antibodies recognising DIAPH1, DIAPH2, DIAPH3 and GAPDH. Compared with the control, the R1213* cases, show reduced intensity of the 155 kDa anti-DIAPH1 immunoreactive band corresponding to full length wild type DIAPH1, but markedly increased intensity of an 80 kDa band, shown by mass spectrometry to contain peptides corresponding to DIAPH1. It was not possible to resolve the relative contributions of wild type and R1213* DIAPH1 to either of these bands. The content of DIAPH2 and DIAPH3 is increased in the cases compared to control. Similar quantities of total protein in the Western blot lanes are indicated by the control blot probed with an antibody recognising GAPDH. (**b**) Confocal microscopy images of poly-L-lysine-immobilised, resting platelets from the cases 10 and 16 and from a control (C), stained for DIAPH1 (cyan), F-actin (red) and α-tubulin (green). DIAPH1 is abnormally distributed throughout the cytoplasm of platelets from the cases. There is an increased F-actin content and number of microtubules with an abnormal distribution in platelets from the cases. Platelets were visualised using a Leica TCS SP5 confocal microscope (Leica Microsystems). Scale bars, 3 μm. (**c**) Representative transmission electron micrographs showing that the microtubules (MT; arrowed) are disorganised and distributed throughout the cytoplasm of platelets from case 10 compared to controls in which microtubules are organised into the marginal band. Images were collected using a EM900 (Carl Zeiss) electron

microscope. Scale bar, 0.5 µm. (**d**) Manual counting of microtubules revealed an increased number of microtubules in platelets from the cases (n=41 platelets) compared with controls (n=104 platelets). Microtubule numbers per platelet are expressed as mean ± s.d. *** indicates $P < 0.001$ by unpaired Student's t-test.

Figure 6: Increased microtubule stability in platelets from R1213* cases: (**a** and **b**) Representative confocal microscopy images of platelets from R1213* cases (10 and 16) and from a control (C) after incubation at 4°C and after subsequent re-warming to 37°C (**a**) or after treatment with the microtubule destabilising toxin colchicine (**b**)**.** F-actin (F-act) is displayed as red and post-translationally modified α-tubulin (ac-tub and Glu-tub) as green. (**c**) Confocal microscopy images of platelets after spreading on fibrinogen (100 µg μL^{-1}). F-act is displayed as red and α-tub, ac-tub or Glu-tub as green. Platelets were visualised using a Leica TCS SP5 confocal microscope (Leica Microsystems). Scale bars, 3µm. (**d**) Western blots of the platelet microtubule cytoskeleton in total protein extract (T) or in pellet (P) or soluble (S) fractions separated by ultracentrifugation, probed with antibodies recognising Tyr-tub, ac-tub or Glu-tub. Data are presented from resting platelets (rest) and after treatment with 10 µM colchicine (colch). (C= healthy control; 10= case 10 and 16= case 16). Equivalent quantities of total platelet extract protein were loaded in each lane.

Figure 7: Overexpression of DIAPH1 R1213* in cell lines reproduces the cytoskeletal alterations in platelets: (**a**) Western blot of protein extracts from HEK293FT cells transfected with DIAPH1 wild-type (WT), DIAPH1 R1213* (R1213*) or empty (C) expression constructs, probed with antibodies recognising the DIAPH1

amino terminus, DIAPH2 or DIAPH3. (**b-d**) Confocal microscopy images of A549 cells transiently transfected with the DIAPH1 R1213* expression construct were stained for DIAPH1 (cyan), F-actin (red) and α-tubulin or acetylated-tubulin (ac-tubulin; green) and with DAPI nuclear counterstain (blue). There was an increased content of F-actin, α-tubulin and ac-tubulin in the cells overexpressing DIAPH1 R1213* compared with adjacent non-transfected cells (**b, c**). Incubation with the FH2 domain inhibitor SMIFH2 reduced F-actin content, but not the content of ac-tubulin (**d**). The cells were visualised using a Leica TCS SP5 confocal microscope (Leica Microsystems). Scale bars, 10 µm. (**e**) Western blots of the microtubule cytoskeleton in total protein extract (T) and in pellet (P) or soluble (S) tubulin fractions separated by ultracentrifugation of the transfected cells, probed with antibodies recognising Tyr-tubulin, ac-tubulin or Glu-tubulin. Incubation with SMIFH2 did not influence the post-translational modification of tubulin, confirming that the DIAPH1 FH2 domain is not critical for the stabilization of microtubules. For the Western blots, there were equivalent total quantities of protein in the cell extracts in each lane confirmed by probing with an antibody recognising β-tubulin (**Supplementary Fig. 12** and **13**).

Pedigree	**1**					**2**		
Case	**10**	**14**	**15**	**16**	**17**	**21**	**22**	**24**
Gender	M	F	M	F	F	F	M	M
Year of birth in 5-year bins	1951-55	1976-80	1976-80	1981-85	1976-80	1976-80	2001-05	2006-10
Platelet count ($x10^9$ L^{-1}; N: 150-400)	69-110	97	140-147	66-114	94-107	63-115	116-129	93
Mean platelet volume (fL; N: 7-9)	13.6	11.2	13.5	13.1-14.1	12.1	13.2	nk	nk
Neutrophil count ($x10^9$ L^{-1}; N:2-7.5)	1.21	1.49	1.66	3.11-3.74	0.9-2.27	1.29-4.34	0.64-1.84	0.62-1.02
Haemoglobin (g dL^{-1}; N: 12-15)	13.2-14.1	12.7	15	12.3-12.5	10.9-12.4	10.2-12.6	11.2-11.8	10.4-10.8
Bleeding score† (<4)	1	1	1	1	1	1	1	1
Type of hearing loss	SN	SN	SN, C	SN	SN	SN	SN	SN
Age of hearing loss (years)	8	2	8	6	6	nk	2	1

Table 1: Characteristics of eight cases with the DIAPH 1 R1213* variant. † bleeding score determined using the International Society of Thrombosis and Haemostasis Bleeding Assessment Tool. Pathological bleeding is associated with bleeding scores >4. NK-not known; SN-sensorineural; C- conductive.

Groups (n)*	Area [µm^2]	Maximal diameter [µm]	Minimal diameter [µm]	% platelets > 4 µm^2
Control (862)	2.53 ± 1.47	2.89 ± 0.67	1.09 ± 0.46	10.90
P10 (99)	3.90 ± 2.50	3.17 ± 0.76	1.51 ± 0.73	31.26
P16 (107)	6.84 ± 4.92	3.77 ± 0.96	2.14 ± 0.91	71.03
P17 (100)	5.48 ± 3.30	3.64 ± 0.90	1.85 ± 0.81	49.00

Table 2. Quantitative morphometric evaluation of platelet size parameters for patients and controls usingelectron microscopy

*n corresponds to the number of platelet sections examined. Data were analyzed for morphometrics parameters.

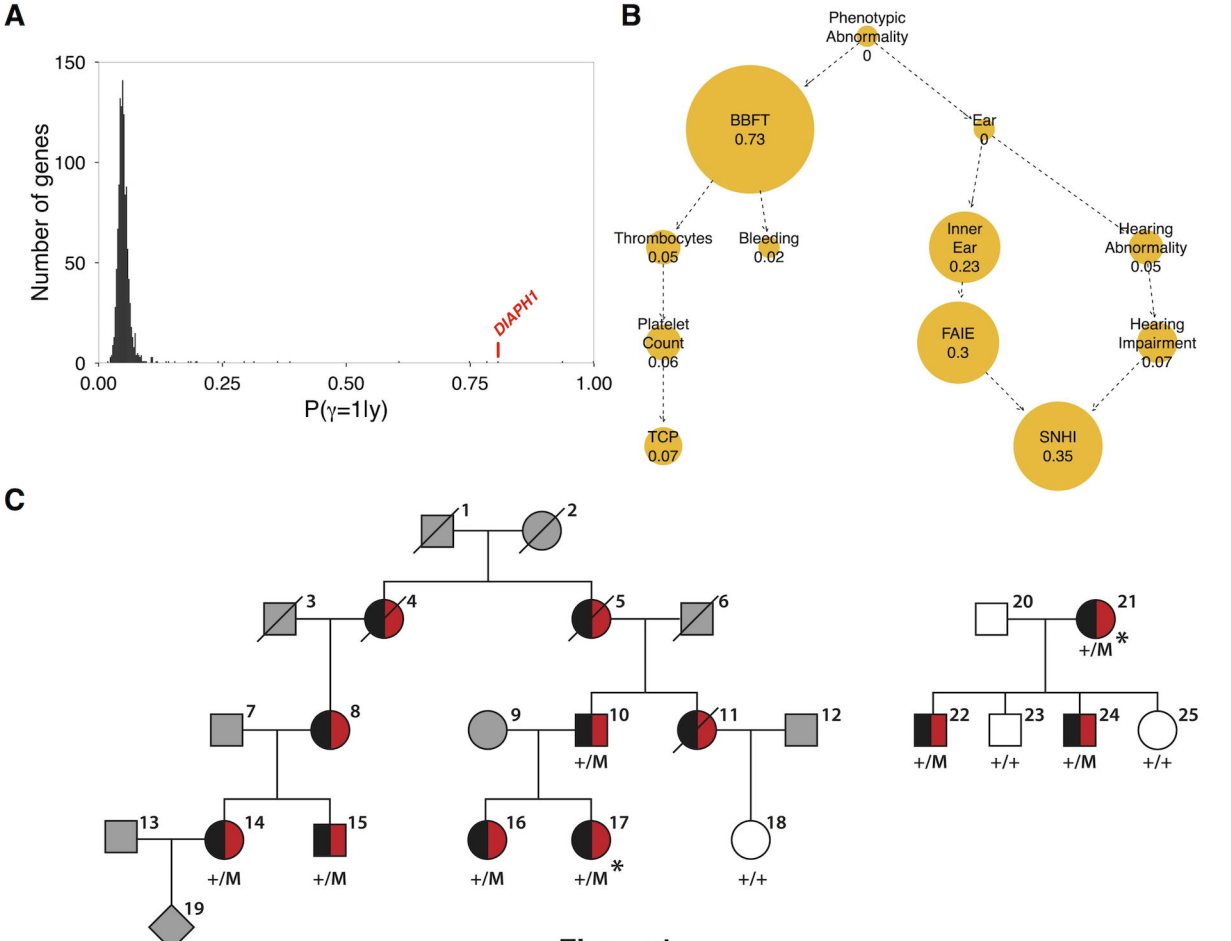
A
Number of genes
150
100
50
0
0.00
0.25
0.50
0.75
1.00
P(γ=1|y)
DIAPH1
B
Phenotypic Abnormality 0
BBFT 0.73
Ear 0
Thrombocytes 0.05
Bleeding 0.02
Inner Ear 0.23
Hearing Abnormality 0.05
Platelet Count 0.06
FAIE 0.3
Hearing Impairment 0.07
TCP 0.07
SNHI 0.35
C
1
2
3
4
5
6
7
8
9
10
+/M
11
12
13
14
+/M
15
+/M
16
+/M
17
+/M*
18
+/+
19
20
21
+/M*
22
+/M
23
+/+
24
+/M
25
+/+

Figure 1

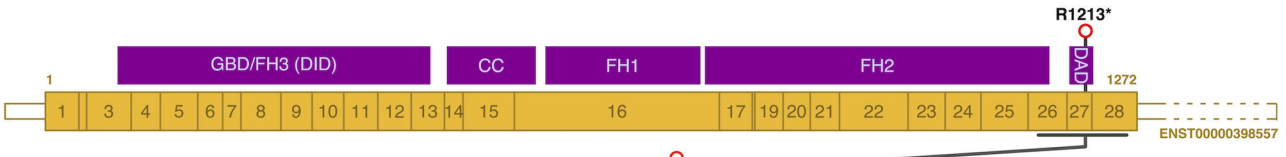
R1213*
GBD/FH3 (DID)
CC
FH1
FH2
DAD
1
1272
1
3
4
5
6
7
8
9
10
11
12
13
14
15
16
17
19
20
21
22
23
24
25
26
27
28
ENST00000398557
Human (O60610) 1158 TEEKMRRAKLAKEKAEKERLEKQQKREQLIDMNAEGDETGVMDSLLEALQSGAAFRRKRGPRQAN--RKAGCAVTSLLASELTKDDAMAAVPAKVSKNSETF-----PTIL 1261
Rat (F1M775) 1106 TEEKMRRAKLAKEKAEKERLEKQQKREQLIDMNAEGDETGVMDSLLEALQSGAAFRRKRGPRQVN--RKAGCAVTSLLASELTKDDAVAASSAKVPKKSEGV-----TTIL 1209
Mouse (O08808) 1141 TEEKMRRAKLAKEKAEKERLEKQQKREQLIDMNAEGDETGVMDSLLEALQSGAAFRRKRGPRQVN--RKAGCAVTSLLASELTKDDAMAPGPVKVPKKSEGV-----PTIL 1244
Cow (F1N0W1) 1162 TEEKMRRAKLAKEKAEKERLEKQQKREQLIDMNAEGDETGVMDSLLEALQSGAAFRRKRGPRQGV--RKAVCAATSQLVSELTKEDAMTCVPAKMPK-SEEV-----PTIL 1264
Fugu (H2TAT5) 1074 AEEKIKRAKLAREKAEKEKEEK-LKRSKLPDMNTGDDETGIMDGLLEALQSGAAFKRKRGPRQAANHRRAGQAVTNILAKELTQEDKPSKPPKKVAEPKLEG----AESLE 1179
Xenopus (F6UXX7) 1173 AEEKMKRAKLAKEKAEKERLEKQQKKEQLIDMNAEGDETGVMDSLLEALNSGAAFRRKRGPRQAN--RKAGCAVTSLLASELTKEDAMTSVPTKKKKPAETDLMETDVGLH 1281
Drosophila (P48608) 988 ELEKKRRLQEAREQSAREQQERQQRKKAVVDMDAPQTQEGVMDSLLEALQTGSAFGQRNR--QARRQRPAGAERRAQLSRSRSRT----RVT-------NGQLMTREMI-- 1083

Figure 2

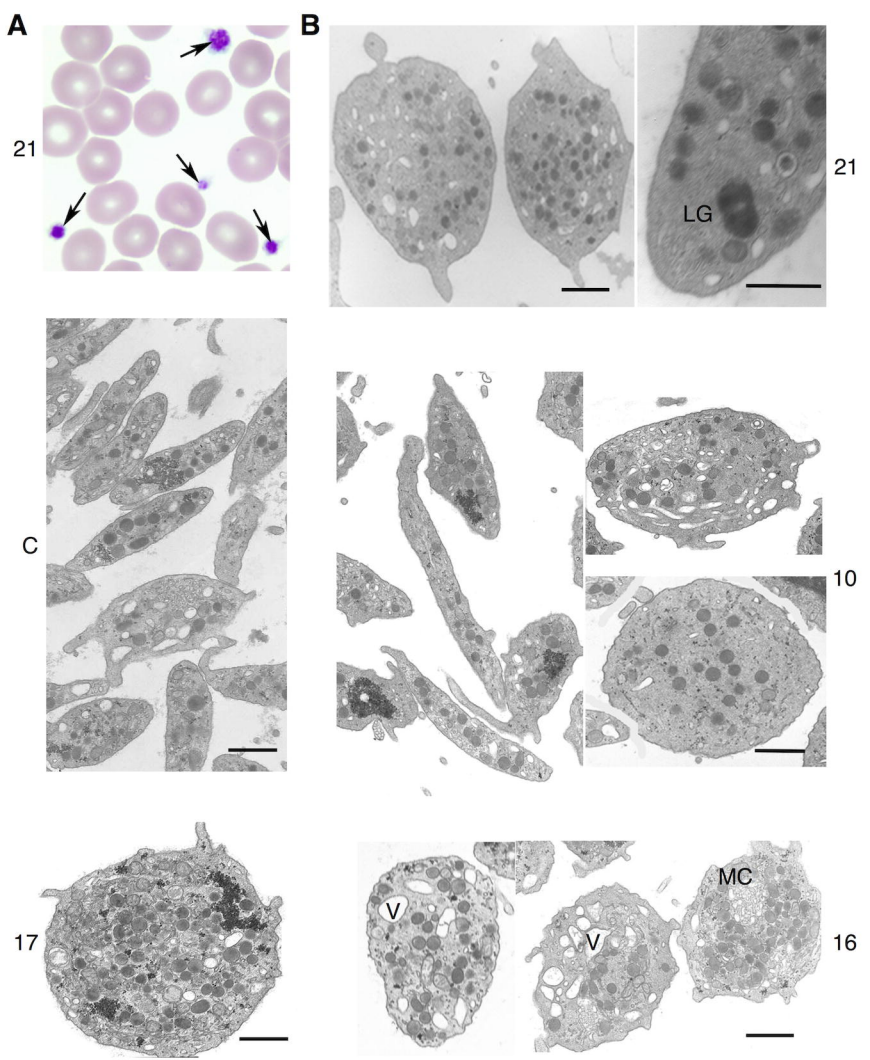

Figure 3

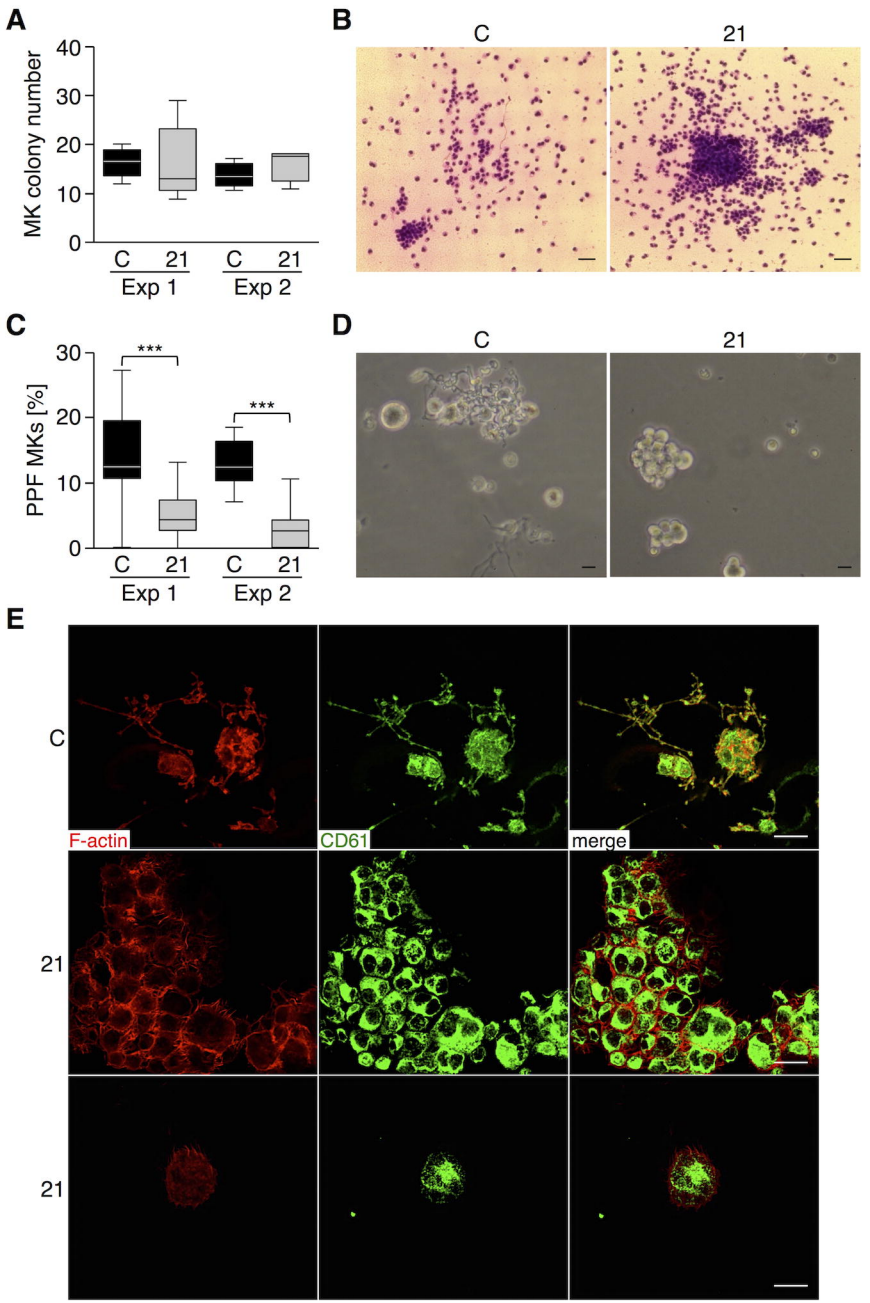
A
MK colony number
40
30
20
10
0
C
21
C
21
Exp 1
Exp 2
B
C
21
C
PPF MKs [%]
***
***
30
20
10
0
C
21
C
21
Exp 1
Exp 2
D
C
21
E
C
F-actin
CD61
merge
21
21

Figure 4

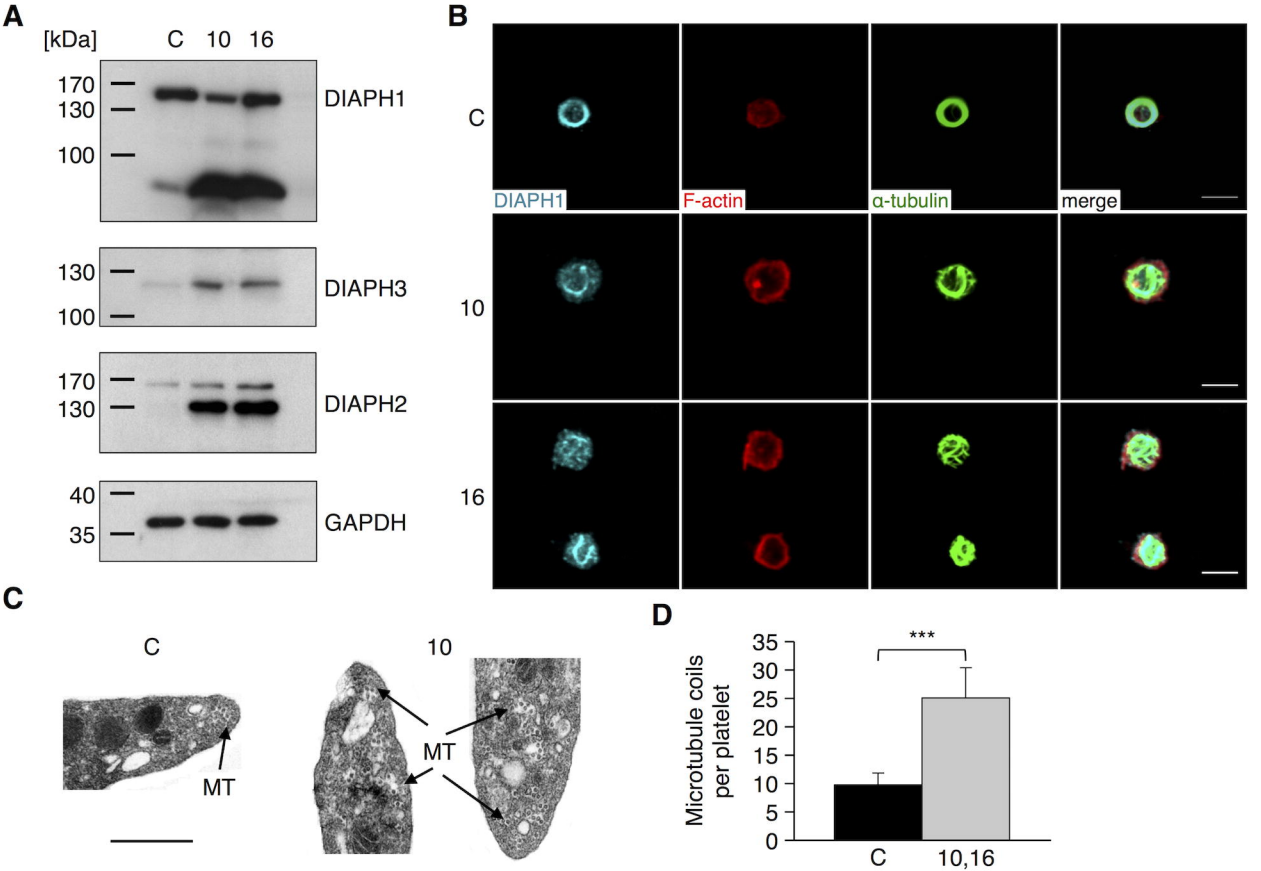
A
[kDa]
C
10
16
170
130
100
DIAPH1
130
100
DIAPH3
170
130
DIAPH2
40
35
GAPDH
B
C
10
16
DIAPH1
F-actin
α-tubulin
merge
C
C
10
MT
MT
D
Microtubule coils per platelet
***
35
30
25
20
15
10
5
0
C
10,16

Figure 5

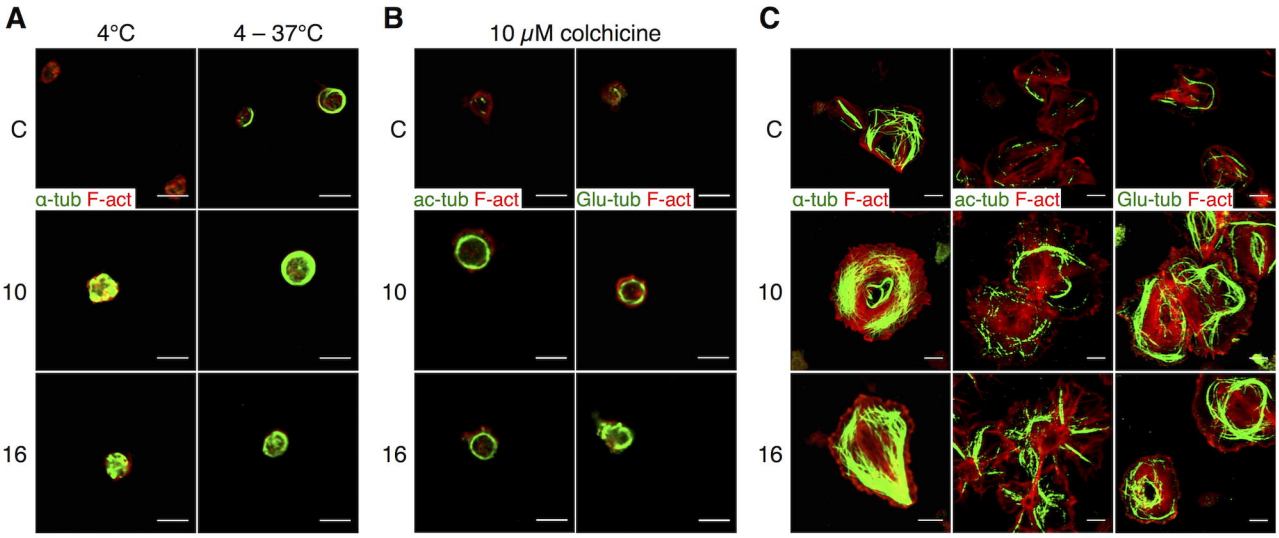
A
4°C
4 – 37°C
C
α-tub F-act
10
16
B
10 μM colchicine
C
ac-tub F-act
Glu-tub F-act
10
16
C
C
α-tub F-act
ac-tub F-act
Glu-tub F-act
10
16

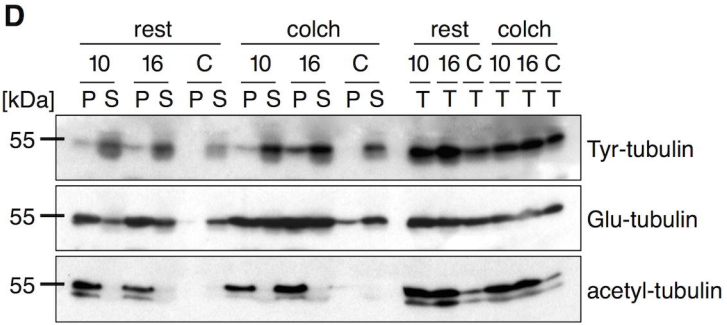
D
rest
colch
rest
colch
10 16 C 10 16 C 10 16 C 10 16 C
[kDa]
P S P S P S P S P S P S T T T T T T
55
Tyr-tubulin
55
Glu-tubulin
55
acetyl-tubulin

Figure 6

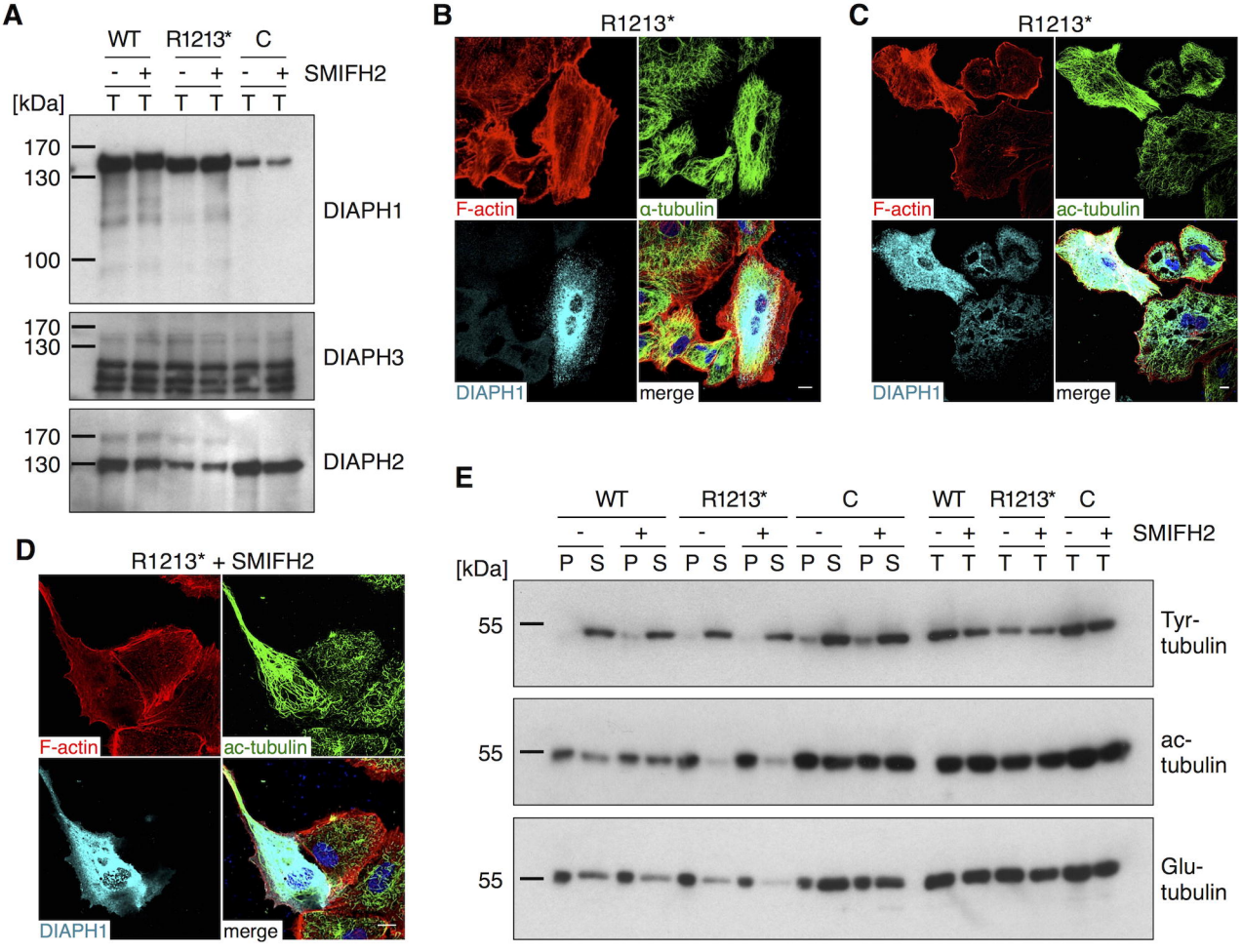
A
WT
R1213*
C
SMIFH2
[kDa]
T T T T T T
170
130
100
DIAPH1
170
130
DIAPH3
170
130
DIAPH2
B
R1213*
F-actin
α-tubulin
DIAPH1
merge
C
R1213*
F-actin
ac-tubulin
DIAPH1
merge
D
R1213* + SMIFH2
F-actin
ac-tubulin
DIAPH1
merge
E
WT
R1213*
C
WT
R1213*
C
SMIFH2
[kDa]
P S P S P S P S P S P S T T T T T T
55
Tyr-tubulin
55
ac-tubulin
55
Glu-tubulin

Figure 7